# Supplementary Material

## 3D Crustal Structure of the Ligurian Sea Revealed by Surface Wave Tomography using Ocean Bottom Seismometer Data

Felix Noah Wolf, Dietrich Lange, Anke Dannowski, Martin Thorwart, Wayne Crawford, Lars Wiesenberg, Ingo Grevemeyer, Heidrun Kopp, and the AlpArray Working Group

Submitted to Solid Earth, April 2021, https://doi.org/10.5194/se-2021-55

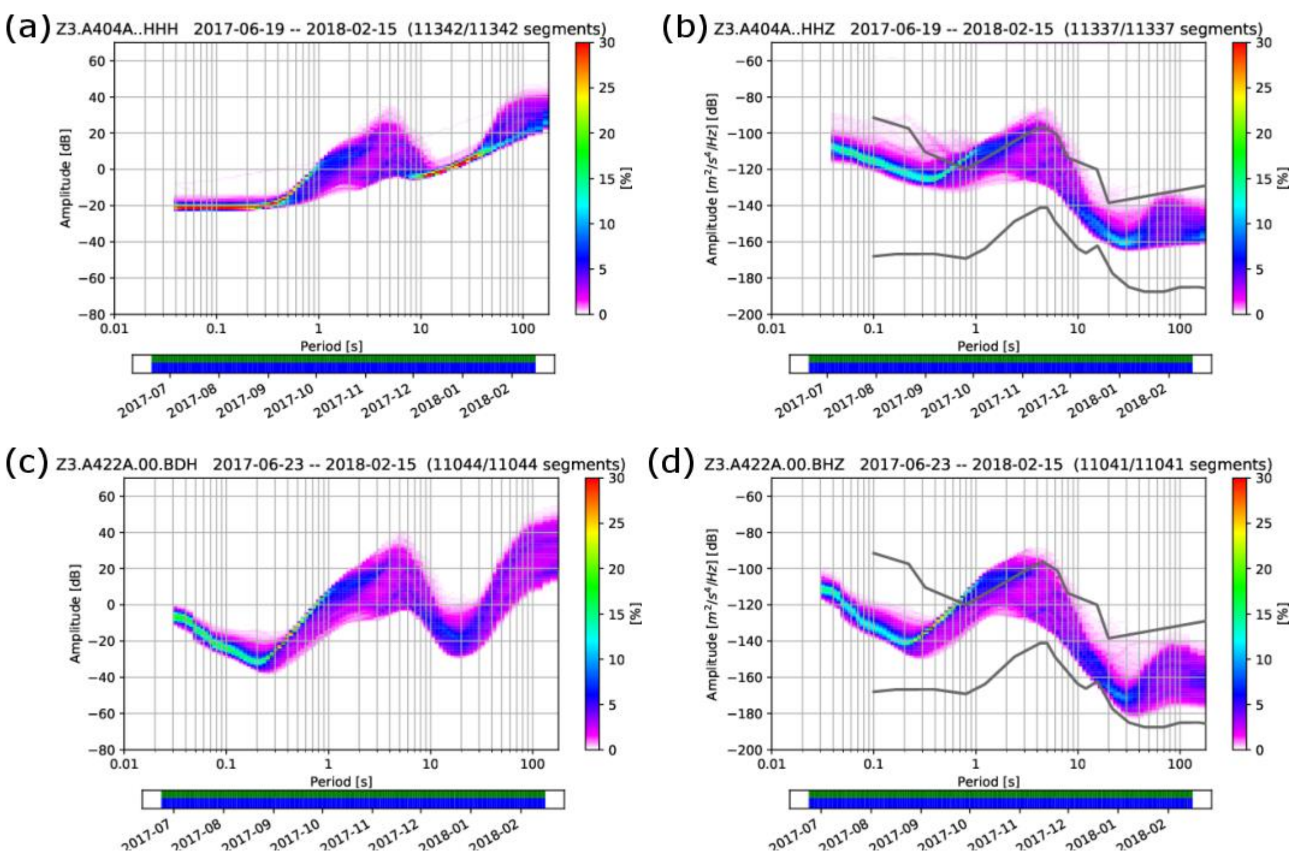


**Figure S1: PPSD plots after McNamara (2004). The top row (a and b) shows instruments on OBS A404A, and the bottom row shows PPSDs of A422A (c and d). The left column shows hydrophone (top) or DPG (bottom), the right column shows vertical seismometer components. Grey lines in b and d are the mean minimum and maximum noise levels for land stations (Peterson, 1993).**

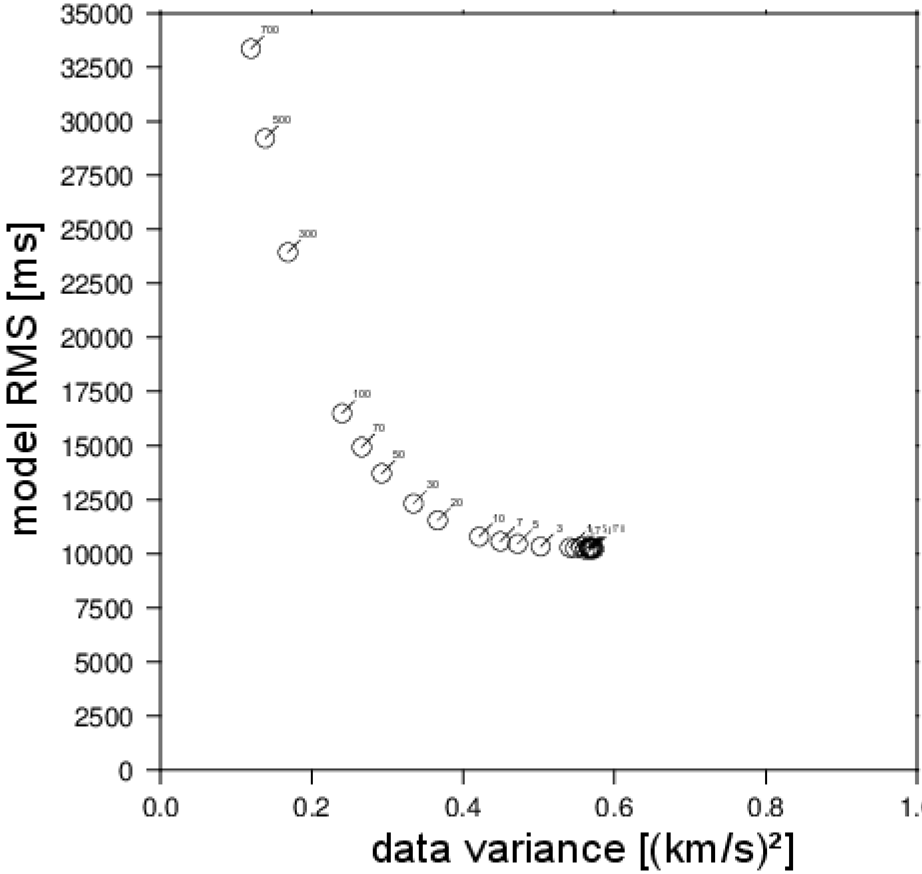


**Figure S2: L-curve for a period of 8 s, fixed smoothing factor (SF = 10) and varied damping factor (DF, labelled in the figure). The data fit (RMS) is plotted against the model roughness (variance). Parameter sets close to the origin of the coordinates provide a reasonable trade-off between model roughness and data fit.**

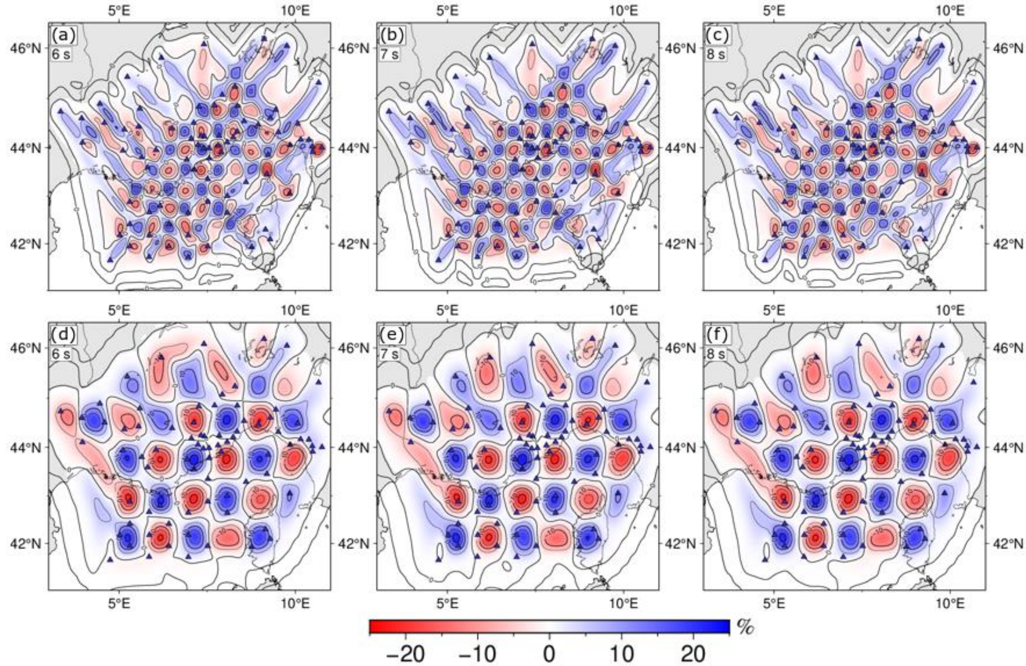


**Figure S3: Checkerboard tests for periods of 6 s, 7 s and 8 s (all ambient noise cross-correlation). The perturbation of the input checkerboard tiles is set to ±25 %. Panels (a)-(c) show checkerboard tests with a grid size of 0.4°x0.4°, panels (d)-(f) show a grid size of 0.8°x0.8°. The standard deviation of Gaussian noise (of travel times) is set to 0.417 s for (a) and (d), 0.458 s for (b) and (e), and 0.5 s for (d) and (h). Blue triangles represent stations.**

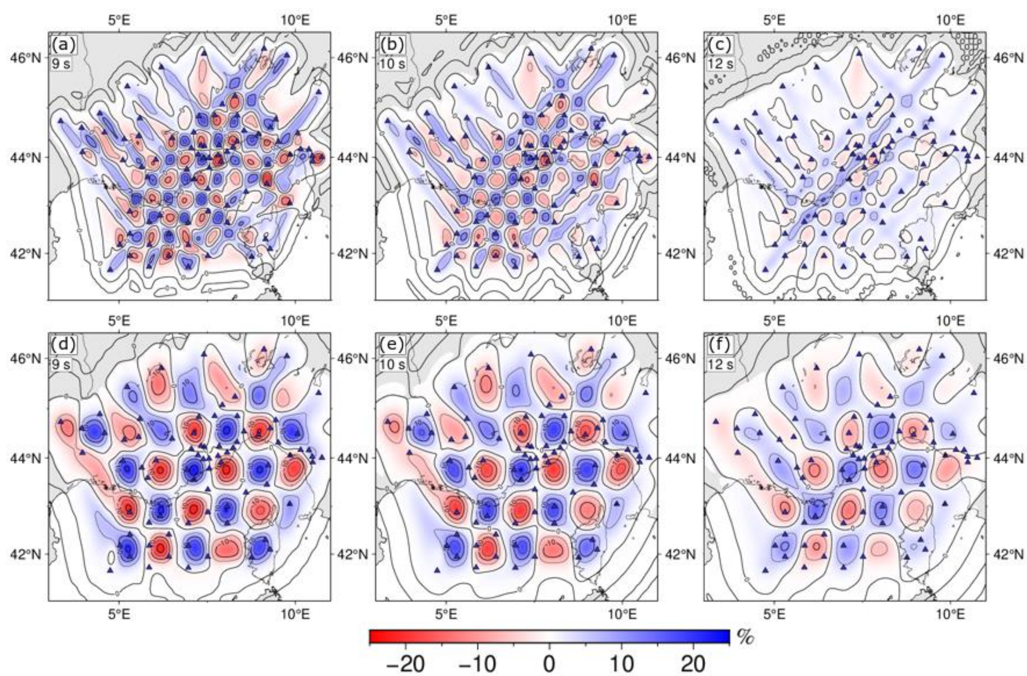

**Figure S4: Same setup as Fig. S4, now for periods of 9 s, 10 s, and 12 s (all ambient noise cross-correlation). The standard deviation of Gaussian noise (of travel times) is set to 0.542 s for (a) and (d), 0.584 s for (b) and (e), and 0.625 s for (d) and (h).**

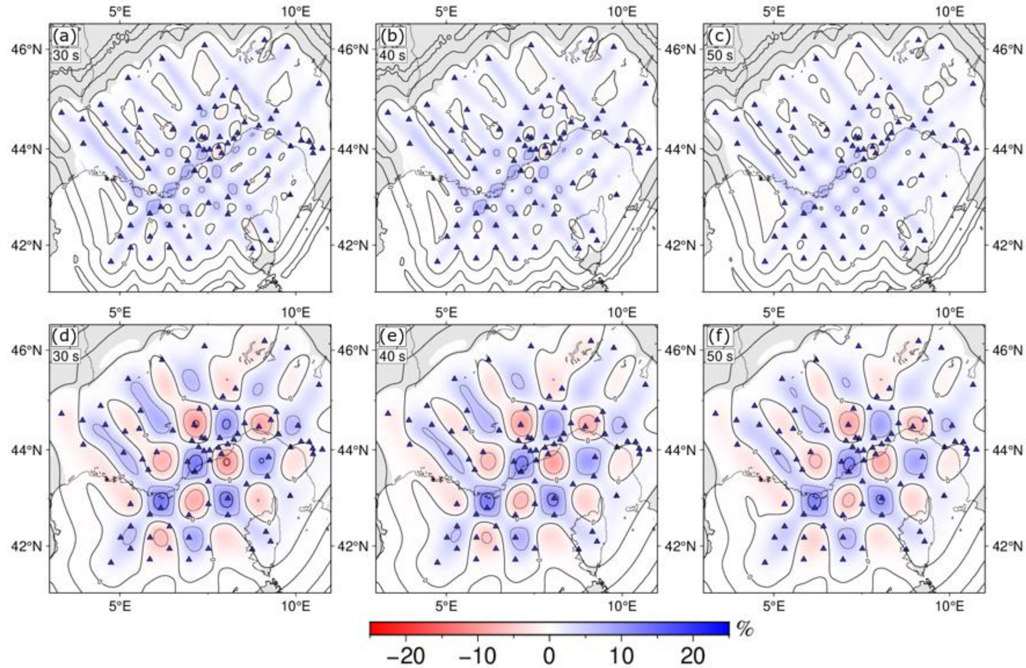


**Figure S5: Same setup as Fig. S4, now for periods of 30 s, 40 s, and 50 s (all teleseismic cross-correlation). The standard deviation of Gaussian noise (of travel times) is set to 0.750 s for (a) and (d), 0.792 s for (b) and (e), and 0.834 s for (d) and (h).**

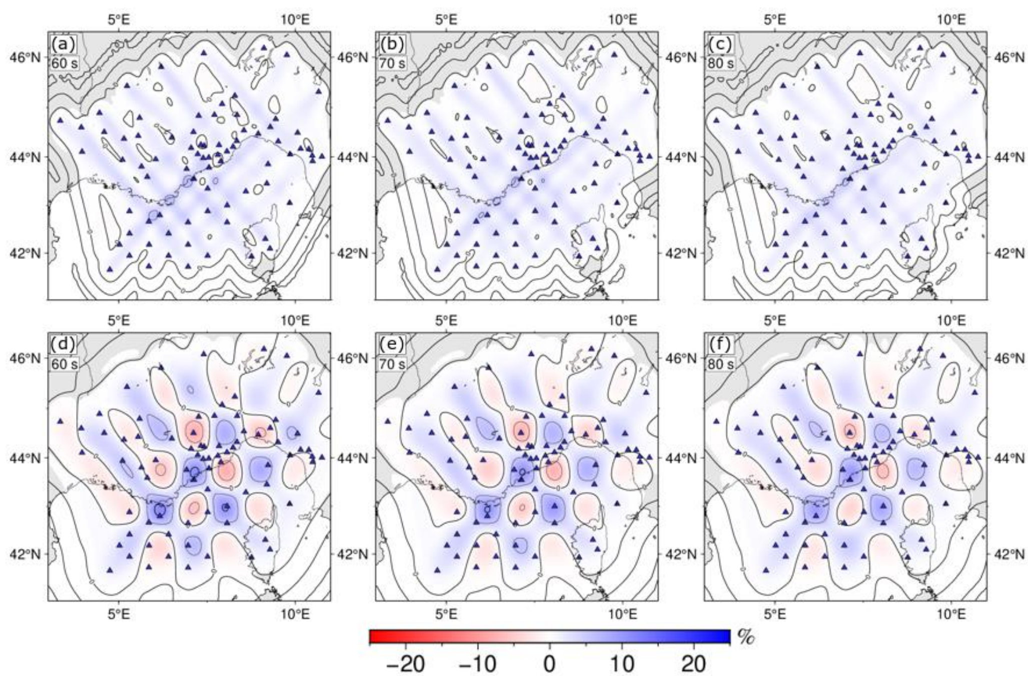

**Figure S6: Same setup as Fig. S4, now for periods of 60 s, 70 s, and 80 s (all teleseismic cross-correlation). The standard deviation of Gaussian noise (of travel times) is set to 0.875 s for (a) and (d), 0.916 s for (b) and (e), and 0.958 s for (d) and (h).**

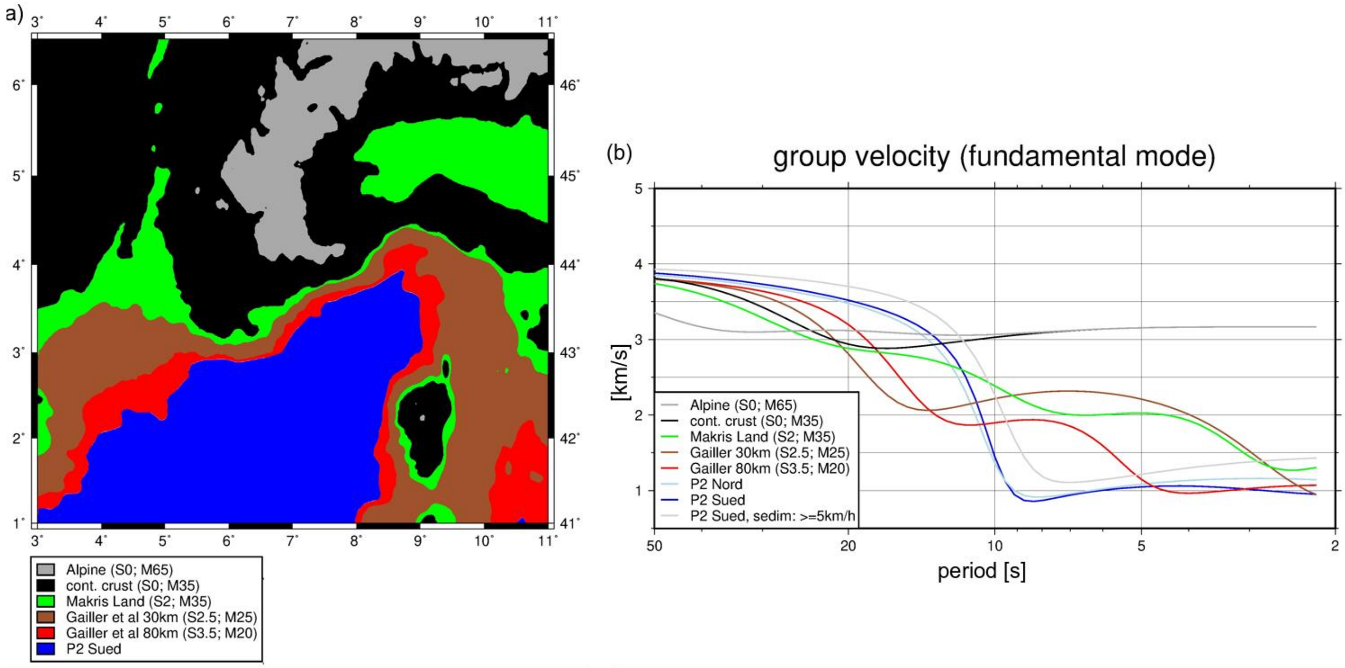


**Figure S7: (a) Synthetic 2D model of the research area used for the restoration test. The coloured areas are assigned to the related group velocity profile shown in (b). 'Makris' refers to Makris et al. (1999), 'Gailler' refers to Gailler et al. (2009).**

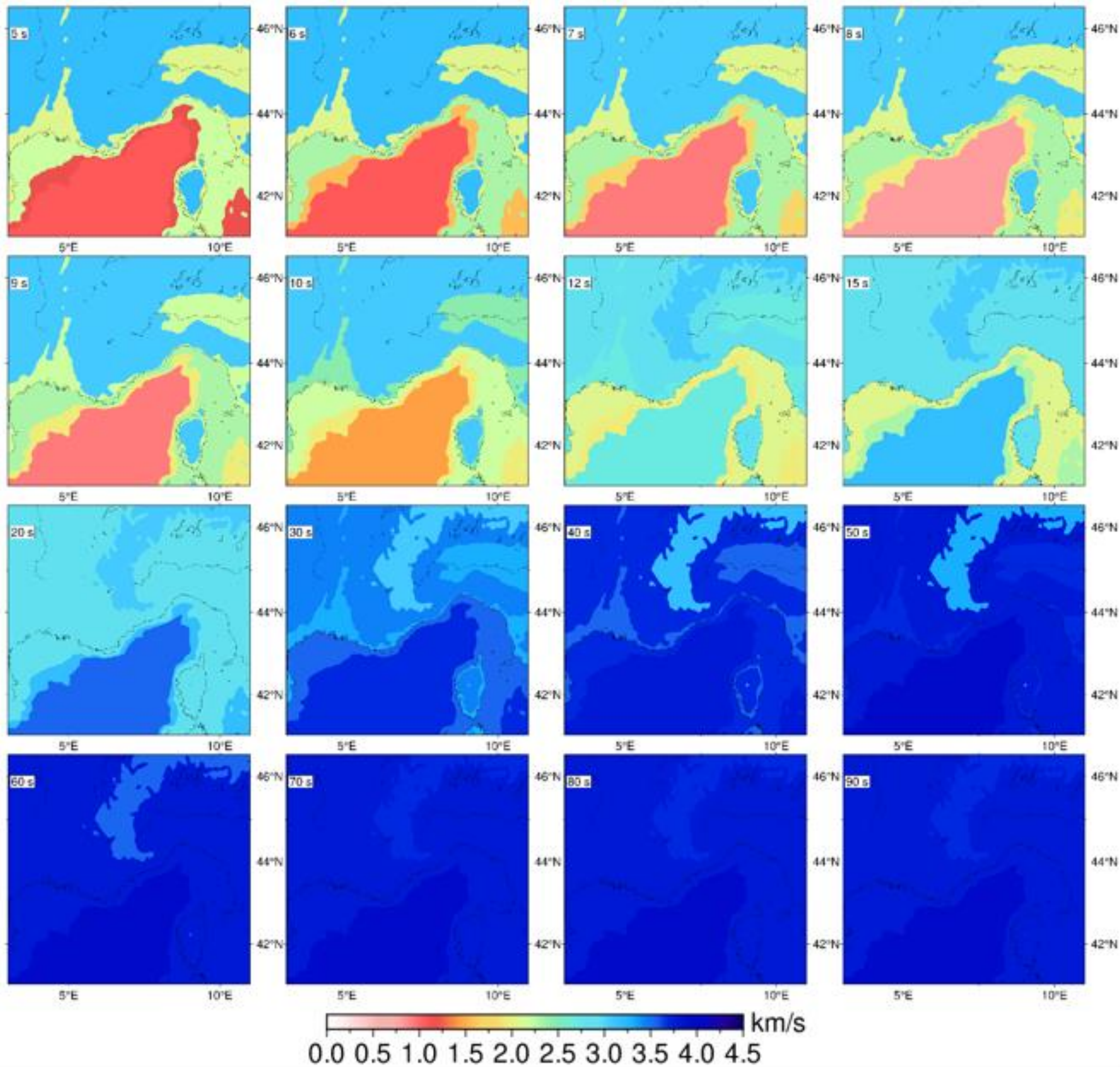


**Figure S8: Theoretical group velocity maps for periods 5 s (top left) to 90 s (bottom right). These are directly derived from the 2D model and assigned velocity profiles shown in Fig. S7.**

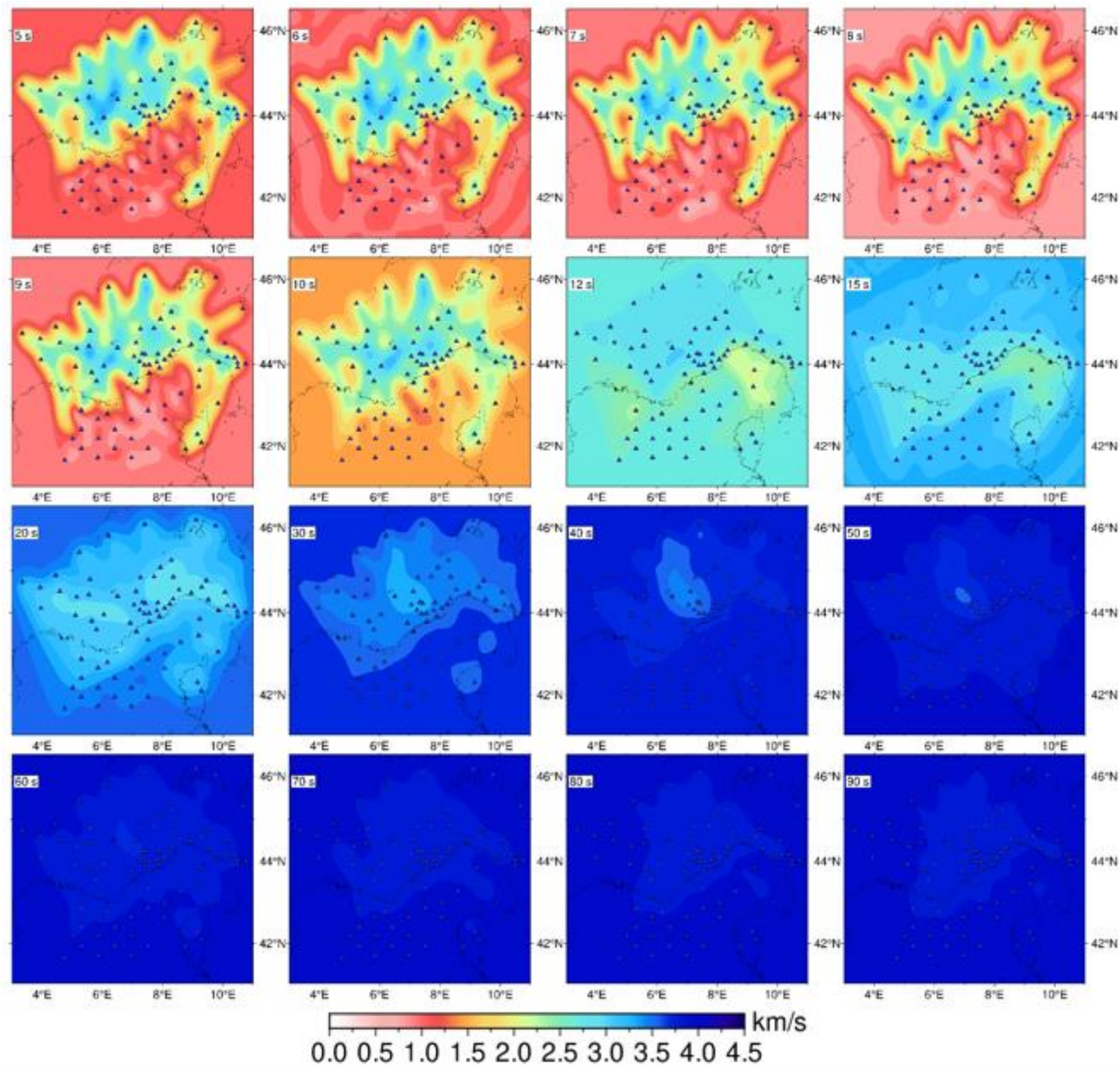


**Figure S9: Group velocity maps (5-90 s) calculated based on the theoretical data derived from the 2D model (Fig. S7). We used the same settings as for the 'real data' tomography. Blue triangles represent stations.**

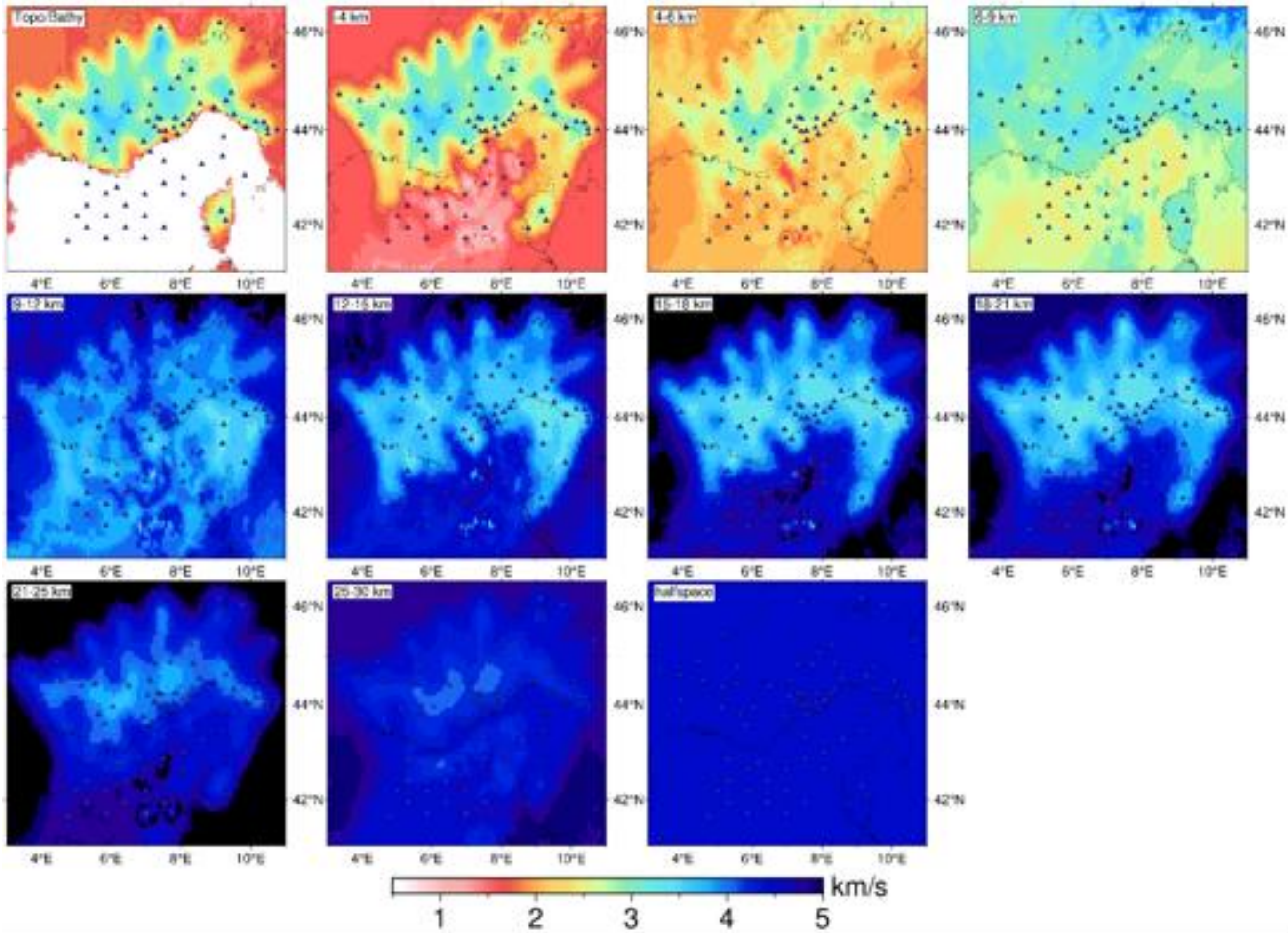


**Figure S10: Shear-wave depth layers, calculated as for the real data set, based on the theoretical group velocities (Fig. S8). Blue triangles represent stations.**

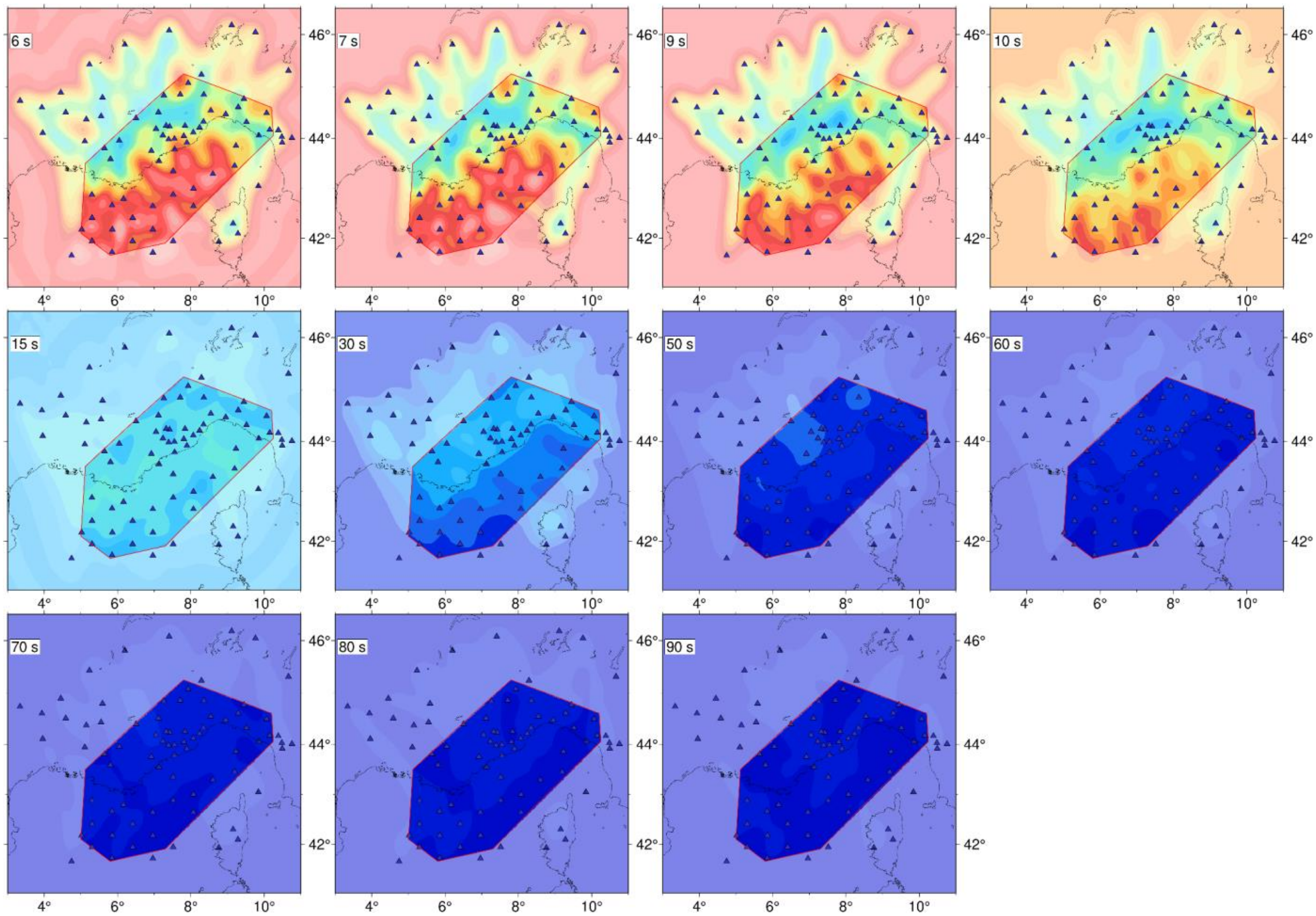


**Figure S11: Group velocity maps of the Ligurian Sea from surface wave tomography. Tomographies for 6-15 s period are based on ambient noise cross-correlation, and tomographies for 30-90 s period are based on the cross-correlation of teleseismic events. A red polygon marks the resolved area. Areas of low resolution are shown in transparent colours; areas without ray coverage show the initial velocity.**

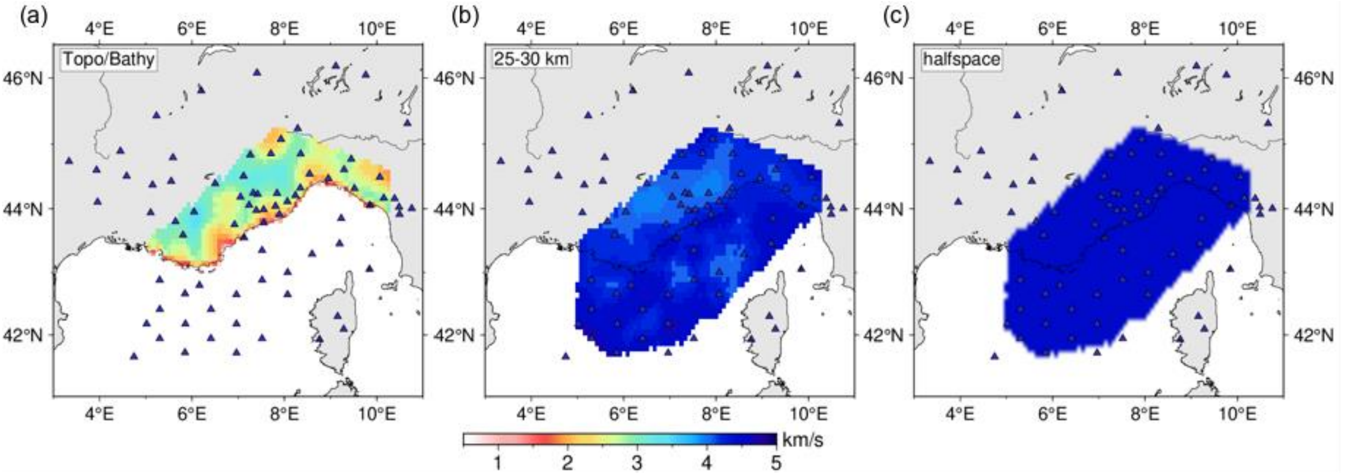


**Figure S12: 2D shear velocity maps resulting from the depth inversion. Layer depth is stated in the upper left corner. Depths (in km) are relative to the sea surface. Layer 1 (a) is set up to show S-wave velocity for layers above sea level onshore and the water column; therefore, there is no $v_S$ offshore in panel (a). The velocity below 30 km (halfspace, panel c) was fixed during the inversion. Blue triangles represent the stations.**

**Table S1: List of all stations used in this study.**

| network | station name | Latitude [°] | Longitude [°] | Elevation [m] |
|---|---|---|---|---|
| Z3 | A402A | 42,8793 | 5,3005 | -1632 |
| Z3 | A404A | 42,1782 | 5,0193 | -2013 |
| Z3 | A405A | 42,4116 | 5,3036 | -2192 |
| Z3 | A406A | 42,6180 | 5,5885 | -2399 |
| Z3 | A409A | 43,3482 | 7,5167 | -1981 |
| Z3 | A412A | 41,6476 | 4,7448 | -2519 |
| Z3 | A413A | 41,9430 | 5,3035 | -2278 |
| Z3 | A414A | 42,1783 | 5,8583 | -2463 |
| Z3 | A415A | 42,4119 | 6,4109 | -2595 |
| Z3 | A416A | 42,6467 | 6,9634 | -2757 |
| Z3 | A417A | 42,8796 | 7,5178 | -2677 |
| Z3 | A418A | 42,9999 | 8,0709 | -2632 |
| Z3 | A419A | 43,2904 | 8,6009 | -2588 |
| Z3 | A420A | 43,4537 | 9,1949 | -1354 |
| Z3 | A421A | 41,7153 | 5,8499 | -2525 |
| Z3 | A422A | 41,9434 | 6,4101 | -2543 |
| Z3 | A423A | 42,1784 | 6,9641 | -2706 |
| Z3 | A425A | 42,6471 | 8,0703 | -2713 |
| Z3 | A428A | 41,7102 | 6,9639 | -2734 |
| Z3 | A429A | 41,9434 | 7,5167 | -2773 |

| | | | | |
|---|---|---|---|---|
| Z3 | A430A | 42,1779 | 7,9809 | -2752 |
| Z3 | A434A | 43,8503 | 9,2299 | -1133 |
| Z3 | A062A | 46,1808 | 9,1126 | 1783 |
| Z3 | A178A | 45,8107 | 6,2004 | 660 |
| Z3 | A184A | 44,8920 | 4,4516 | 750 |
| Z3 | A186B | 44,7930 | 5,5892 | 978 |
| Z3 | A187A | 44,7343 | 3,3398 | 935 |
| Z3 | A188A | 44,6001 | 3,9367 | 1085 |
| Z3 | A192A | 44,5069 | 4,5869 | 249 |
| Z3 | A193A | 44,3711 | 5,1476 | 390 |
| Z3 | A194A | 44,3933 | 6,5023 | 1255 |
| Z3 | A215A | 45,4307 | 5,2323 | 450 |
| Z3 | A216A | 44,4291 | 5,5499 | 1245 |
| Z3 | A281A | 44,8534 | 7,7099 | 292 |
| Z3 | A283B | 45,2380 | 8,2885 | 195 |
| Z3 | A289A | 46,0473 | 9,7610 | 1780 |
| Z3 | A313A | 45,3135 | 10,6628 | 64 |
| Z3 | A317A | 43,0499 | 9,8424 | 35 |
| GU | BHB | 44,8352 | 7,2633 | 585 |
| IV | BOB | 44,7679 | 9,4478 | 910 |
| GU | BURY | 43,7825 | 7,5569 | 20 |
| GU | CANO | 44,2075 | 8,2372 | 638 |
| GU | CARD | 44,0261 | 10,4821 | 380 |
| CH | DIX | 46,0801 | 7,4082 | 2410 |
| GU | ENR | 44,2267 | 7,4203 | 1160 |
| GU | EQUI | 44,1660 | 10,1530 | 350 |
| GU | GBOS | 44,2416 | 7,8399 | 897 |
| GU | GORR | 44,6071 | 9,2926 | 609 |
| GU | GRAM | 44,4913 | 10,0658 | 850 |
| IV | IMI | 43,9105 | 7,8932 | 840 |
| GU | MAIM | 43,9142 | 10,4915 | 200 |
| GU | MGRO | 44,0424 | 7,8081 | 1689 |
| IV | MONC | 45,0739 | 7,9271 | 480 |
| IV | MSSA | 44,3163 | 9,5174 | 930 |
| GU | PCP | 44,5413 | 8,5452 | 770 |
| IV | PLMA | 44,0498 | 9,8537 | 22 |
| GU | POPM | 44,0045 | 10,7570 | 440 |
| GU | PZZ | 44,5068 | 7,1160 | 1430 |
| IV | QLNO | 44,3243 | 8,3459 | 547 |

| | | | | |
|---|---|---|---|---|
| GU | RNCA | 44,4712 | 8,9512 | 235 |
| GU | RORO | 44,1122 | 8,0662 | 260 |
| GU | ROTM | 44,8493 | 8,3527 | 221 |
| GU | STV | 44,2455 | 7,3260 | 930 |
| MN | VLC | 44,1594 | 10,3864 | 555 |
| FR | AJAC | 41,9279 | 8,7630 | 27 |
| FR | ARBF | 43,4917 | 5,3325 | 185 |
| FR | ARTF | 43,5882 | 5,8067 | 510 |
| FR | ASEAF | 42,7948 | 6,1635 | 2470 |
| FR | BLAF | 43,9510 | 6,0450 | 590 |
| FR | BSTF | 43,8009 | 5,6433 | 500 |
| FR | CALF | 43,7528 | 6,9218 | 1242 |
| FR | CORF | 42,298 | 9,1530 | 475 |
| FR | EILF | 43,5479 | 7,1312 | 30 |
| FR | ISO | 44,1840 | 7,0500 | 910 |
| FR | SAOF | 43,9860 | 7,5532 | 595 |
| FR | SAUF | 43,9377 | 5,1064 | 230 |
| FR | SMPL | 42,0945 | 9,2847 | 405 |
| FR | SPIF | 44,0558 | 7,2366 | 1380 |
| FR | TRBF | 44,1054 | 3,9587 | 120 |
| FR | TURF | 43,9749 | 7,3919 | 1650 |

**Table S2: Number of station pairs per period and background velocity for FMST.**

| **Period** | **traveltimes used** | **initial velocity [km/s]** | **pick error [s] (estimated)** | **final RMS [s]** |
|---|---|---|---|---|
| 5 | 843 | 1.05 | ±0.750 | 11.21 |
| 6 | 872 | 1.00 | ±0.833 | 11.33 |
| 7 | 891 | 0.94 | ±0.917 | 12.08 |
| 8 | 890 | 0.87 | ±1.000 | 11.79 |
| 9 | 861 | 0.91 | ±1.083 | 11.50 |
| 10 | 846 | 1.44 | ±1.167 | 10.15 |
| 12 | 881 | 2.72 | ±1.250 | 8.73 |

| | | | | |
|---|---|---|---|---|
| 15 | 741 | 3.25 | ±2.333 | 8.40 |
| 20 | 955 | 3.52 | ±1.417 | 5.07 |
| 30 | 1026 | 3.73 | ±1.500 | 4.62 |
| 40 | 999 | 3.83 | ±1.583 | 4.11 |
| 50 | 973 | 3.90 | ±1.667 | 4.00 |
| 60 | 899 | 3.90 | ±1.750 | 4.17 |
| 70 | 817 | 3.90 | ±1.833 | 4.75 |
| 80 | 703 | 3.90 | ±1.917 | 5.32 |
| 90 | 602 | 3.90 | ±2.000 | 5.21 |

**Table S3: FMST parameter settings. We only state settings that were changed from their default values.**

| | |
|---|---|
| number of iterations | 10 |
| N-S range of grid (degrees) | 46.5-41 |
| W-E range of grid (degrees) | 3-11 |
| number of grid points in theta (N-S)* | 28 |
| number of grid points in phi (E-W)* | 35 |
| background velocity (km $s^{-1}$) | period dependent (see S2) |
| damping factor (epsilon) | 20 for periods ≦ 15 s; 10 else |
| smoothing factor (eta) | 10 |
| checkerboard (optional): | |
| maximum perturbation of vertices | 25 % |
| checkerboard size (NxN grid cells) | 2 |

* The grid gets refined during the tomography. The outcome is a grid of 406x511 grid points.

**Table S4: Starting model for 1D depth inversion. The inversion tool solves for $v_S$, $v_P$ is calculated using $v_P/v_S$ = 1.78.**

| | **Onshore model** | **Offshore model** |
|---|---|---|
| Layer 1 | Topography to sea surface; | Sea surface to seafloor; $v_P$=1.52 km $s^{-1}$, |

| | | |
|---|---|---|
| | $v_S$=2.2472 km $s^{-1}$ | $v_S$=0 km $s^{-1}$ (fixed) |
| Layer 2 | Sea surface – 4 km; $v_S$=2.2472 km $s^{-1}$ | Seafloor – 4 km; $v_S$=1.4045 km $s^{-1}$ |
| Layer 3 | 4-6 km; $v_S$=2.2472 km $s^{-1}$ | |
| Layer 4 | 6-9 km; $v_S$=3.0809 km $s^{-1}$ | |
| Layer 5 | 9-12 km; $v_S$=4.2135 km $s^{-1}$ | |
| Layer 6 | 12-15 km; $v_S$=4.2135 km $s^{-1}$ | |
| Layer 7 | 15-18 km; $v_S$=4.2135 km $s^{-1}$ | |
| Layer 8 | 18-21 km; $v_S$=4.2135 km $s^{-1}$ | |
| Layer 9 | 21-25 km; $v_S$=4.6 km $s^{-1}$ | |
| Layer 10 | 25-30 km; $v_S$=4.6 km $s^{-1}$ | |
| Layer 11 | halfspace; $v_S$=4.6 km $s^{-1}$ (fixed) | |